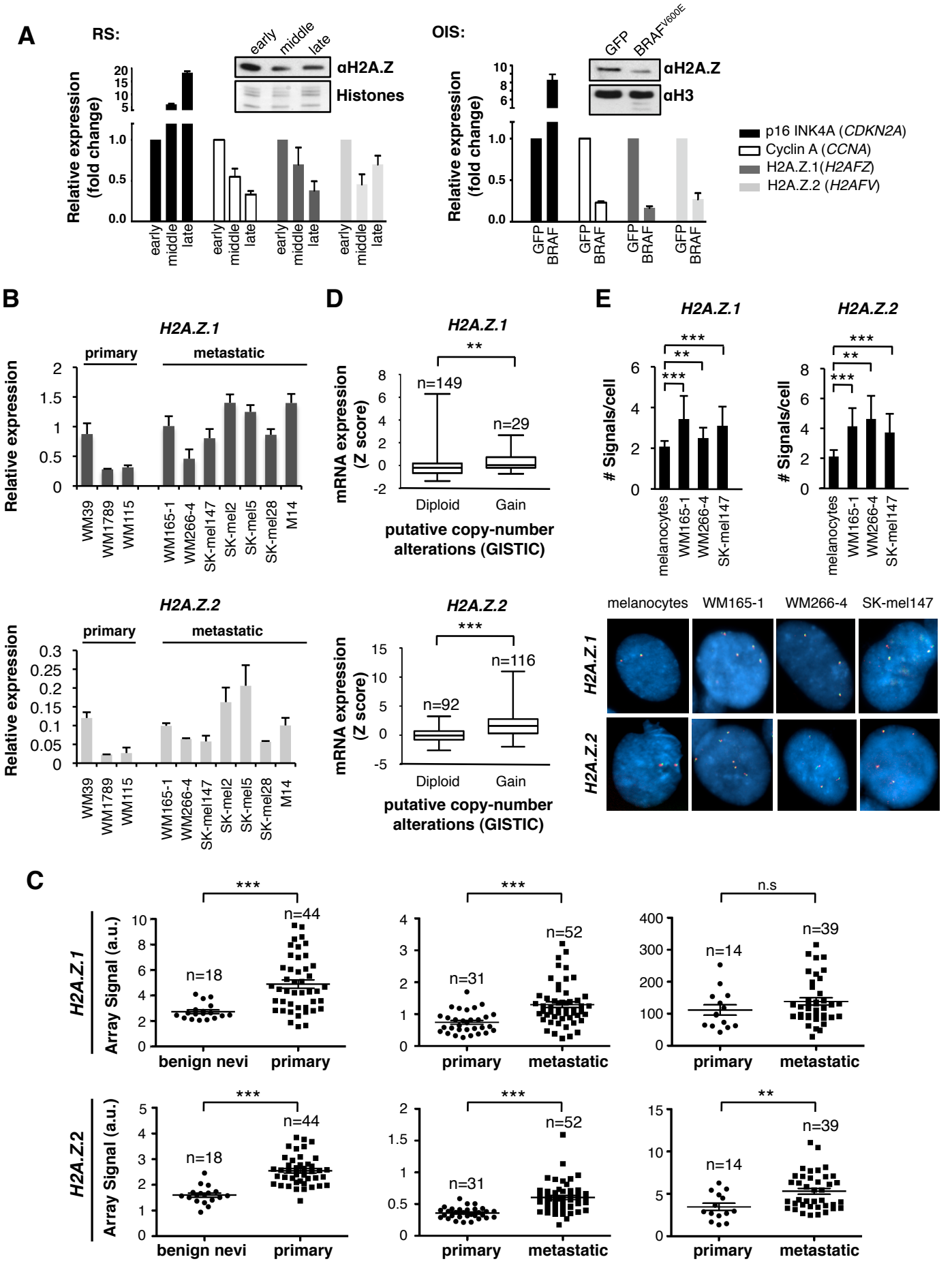
A
RS:
early
middle
late
αH2A.Z
Histones
Relative expression (fold change)
OIS:
GFP
BRAFV600E
αH2A.Z
αH3
p16 INK4A (CDKN2A)
Cyclin A (CCNA)
H2A.Z.1(H2AFZ)
H2A.Z.2 (H2AFV)
B
H2A.Z.1
primary
metastatic
Relative expression
WM39
WM1789
WM115
WM165-1
WM266-4
SK-mel147
SK-mel2
SK-mel5
SK-mel28
M14
H2A.Z.2
D
H2A.Z.1
mRNA expression (Z score)
n=149
n=29
Diploid
Gain
putative copy-number alterations (GISTIC)
H2A.Z.2
n=92
n=116
E
H2A.Z.1
H2A.Z.2
Signals/cell
melanocytes
WM165-1
WM266-4
SK-mel147
C
H2A.Z.1
H2A.Z.2
Array Signal (a.u.)
n=18
n=44
benign nevi
primary
n=31
n=52
metastatic
n=14
n=39
n.s

Figure S1. H2A.Z.1 and H2A.Z.2 are overexpressed with increased copy number in metastatic melanoma. Related to Figure 1.

(A) H2A.Z immunoblot and isoform-specific qRT-PCR of growing and senescent melanocytes. Both replicative senescence (RS) and oncogene-induced senescence (OIS) were assessed. Early, middle, late represent passages 4, 6 and 8, respectively. Senescence was monitored by expression levels of $p16^{INK4A}$ and Cyclin A. Values are normalized to expression of GAPDH. Mean ± SD (n=3). H3 and histones used for immunoblot loading; note the cleaved forms of H3 as marker of senescence (Duarte et al., 2014).

(B) Isoform-specific qRT-PCR (H2A.Z.1 (top), H2A.Z.2 (bottom)) of a panel of primary and metastatic melanoma cell lines. Values are normalized to expression of GAPDH. Mean ± SD (n=3).

(C) Microarray expression levels of H2A.Z.1 (top) and H2A.Z.2 (bottom) in benign nevi, primary and metastatic melanomas (from left to right: GEOD3189 (Talantov et al., 2005); GSE7553 (Riker et al., 2008); GSE8401 (Xu et al., 2008)). Mann Whitney test (two-tailed); Asterisks as follows in all Supplementary Figures: *p<0.05, **p<0.01, ***p<0.001.

(D) H2A.Z.1 and H2A.Z.2 expression (RNA-sequencing) in diploid melanoma patients versus patients harboring increased copy number. The Z score was calculated from cBioPortal by normalizing the mRNA expression values to the average of the reference samples. All patient samples in the database have CNA (Copy Number Analysis), mRNA expression and sequencing data available at http://www.cbioportal.org. Mann-Whitney test (two-tailed).

(E) A subset of cell lines from (B) and primary foreskin-derived melanocytes were subjected to FISH with *H2AFZ* and *H2AFV* probes. Representative images are shown on the left; two probes (red and green, 5' and 3') were used for each gene. Signals were counted in ≥25 cells and plotted (right). Mean ± SD is shown. Mann-Whitney test (two-tailed).

Vardabasso et al_Suppl. Figure 2

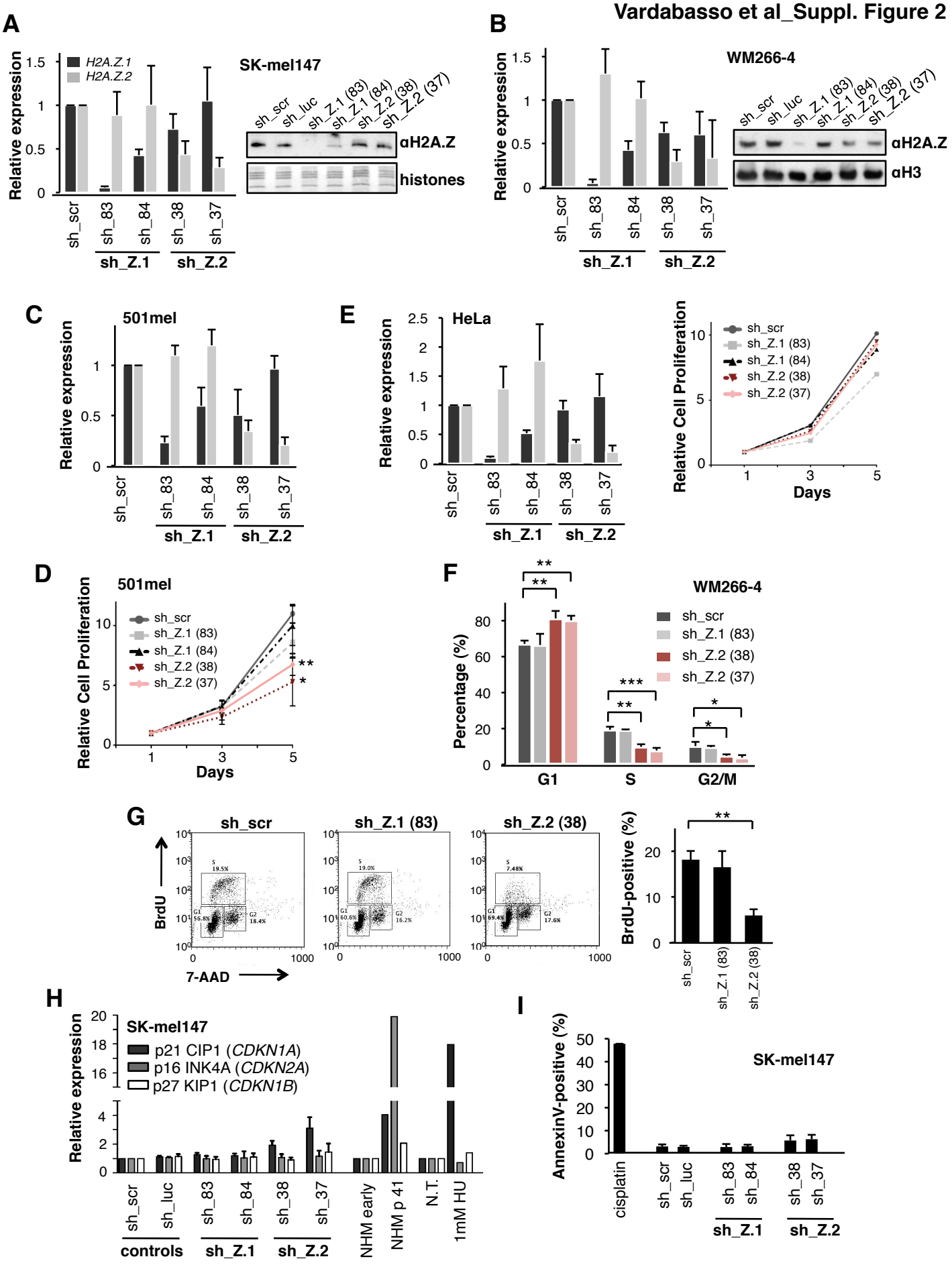

Figure S2. H2A.Z.2 depletion impairs melanoma cell growth without triggering cell death or senescence. Related to Figure 2.

(A),(B),(C) qRT-PCR of relative H2A.Z.1 and H2A.Z.2 expression and/or H2A.Z immunoblot of whole-cell extracts from SK-mel147 (A), WM266-4 (B) and 501mel (C) melanoma cells stably transduced with non-targeting scrambled (sh_scr) control, or H2A.Z.1 (sh_83, sh_84) and H2A.Z.2 (sh_38, sh_37) shRNAs. For qRT-PCR, values are normalized to GAPDH, and relative to scrambled shRNA. Mean ± SD is shown (n≥3). For immunoblot, H3 or histones used for loading.

(D) Proliferation assay of 501mel cells expressing shRNAs as in (A-C). Proliferation curves of control and isoform-specific-depleted cells are shown. Mean ± SD is shown (n≥3). Two-way ANOVA.

(E) (Left) qRT-PCR of HeLa cells transduced with shRNAs as in (A-C) to monitor relative mRNA expression levels of H2A.Z.1 and H2A.Z.2. Values are normalized to GAPDH, and relative to scrambled shRNA. Mean ± SD is shown (n≥3). (Right) HeLa cells were counted up to 5 days after plating and normalized proliferation curves of control and H2A.Z isoform-specific-depleted cells are represented. One representative experiment is shown. Two-way ANOVA; note that H2A.Z loss doesnot alter proliferation.

(F) Percentage of WM266-4 in G1, S or G2/M phases, as revealed by PI incorporation. Values are mean ± SD (n≥3); unpaired Student's test (two-tailed).

(G) Cell cycle analyses of WM266-4 cells expressing scrambled or shRNAs against H2A.Z.1 (83) or H2A.Z.2 (38). Cells were pulsed with BrdU for flow cytometry analysis. Replicating and nonreplicating cells are distinguished using BrdU and 7-AAD staining. Profiles from one representative experiment are displayed. Cell cycle phases were gated and percentages depicted. BrdU-positive S phase cells are shown as mean values ± SD (n≥3) (right); unpaired Student's test (two-tailed).

(H) Expression of CDK inhibitors commonly upregulated in cellular senescence was analyzed by qRT-PCR upon H2A.Z isoform-specific knock down. Late passage (p41) senescent normal human melanocytes (NHM) vs. early passage NHM, and Hydroxyurea (1mM for 24 hours) treated SK-mel147 vs. not treated (N.T.) cells were used as positive controls. Expression is shown normalized to B-actin and relative to scrambled shRNA. Mean ± SD is shown (n≥3).

(I) Control and H2A.Z.1/H2A.Z.2-depleted SK-mel147 were subjected to Annexin V staining and analyzed by flow cytometry to detect apoptotic cells. Cells treated with 20 μM cisplatin (24 hours) were used as positive control. Mean ± SD are shown (n≥3).

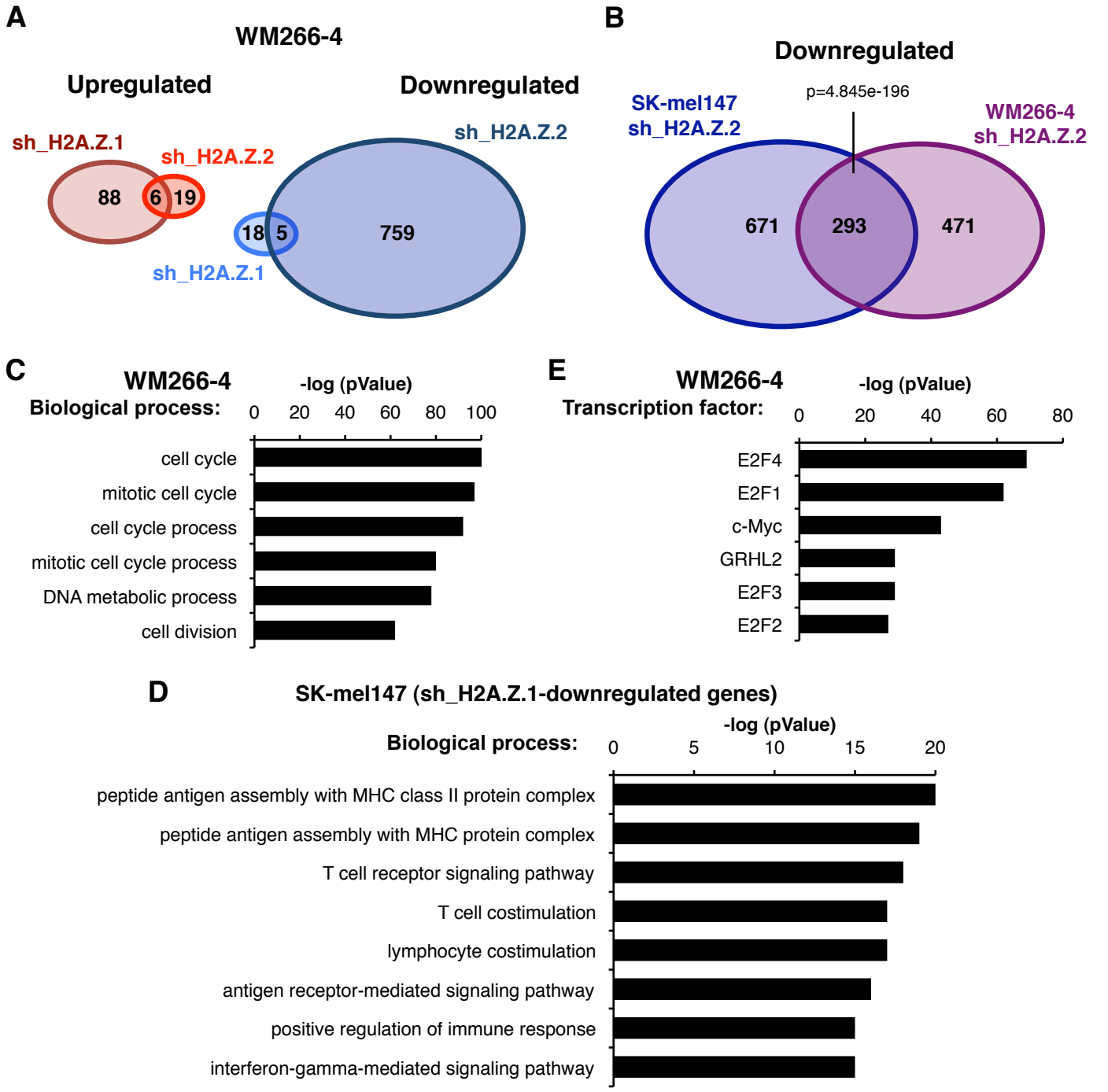

Figure S3. H2A.Z. isoforms control gene expression of distinct regulatory pathways. Related to Figure 3.

(A) Venn diagrams displaying up- and downregulated genes upon H2A.Z.1 and H2A.Z.2 knock down in WM266-4 $BRAF^{V600E}$-mutant melanoma cells. Genes displaying a significant (lfdr<0.2) change are shown, and calculated as an average of two shRNAs per H2A.Z isoform relative to an average of two non-targeting control shRNAs (scr and luc). See Table S1 for gene lists.

(B) Overlap of downregulated genes upon H2A.Z.2 knock down from microarrays of SKmel-147 and WM266-4; hypergeometric test used to generate p-value. See Table S1 for the list of overlapping genes.

(C) Functional annotation of genes downregulated upon H2A.Z.2 knock down in WM266-4 cells (n=764). Enriched groups are ranked by the most significant p value; analysis performed with MetaCore.

(D) Functional annotation of genes downregulated upon H2A.Z.1 loss in SK-mel147 cells (n=180). Enriched groups are ranked by the most significant p value; analysis performed with MetaCore.

(E) Transcription factor regulation of genes downregulated upon H2A.Z.2 knock down in WM266-4 cells. Enriched groups are ranked by the most significant p value; analysis performed with MetaCore.

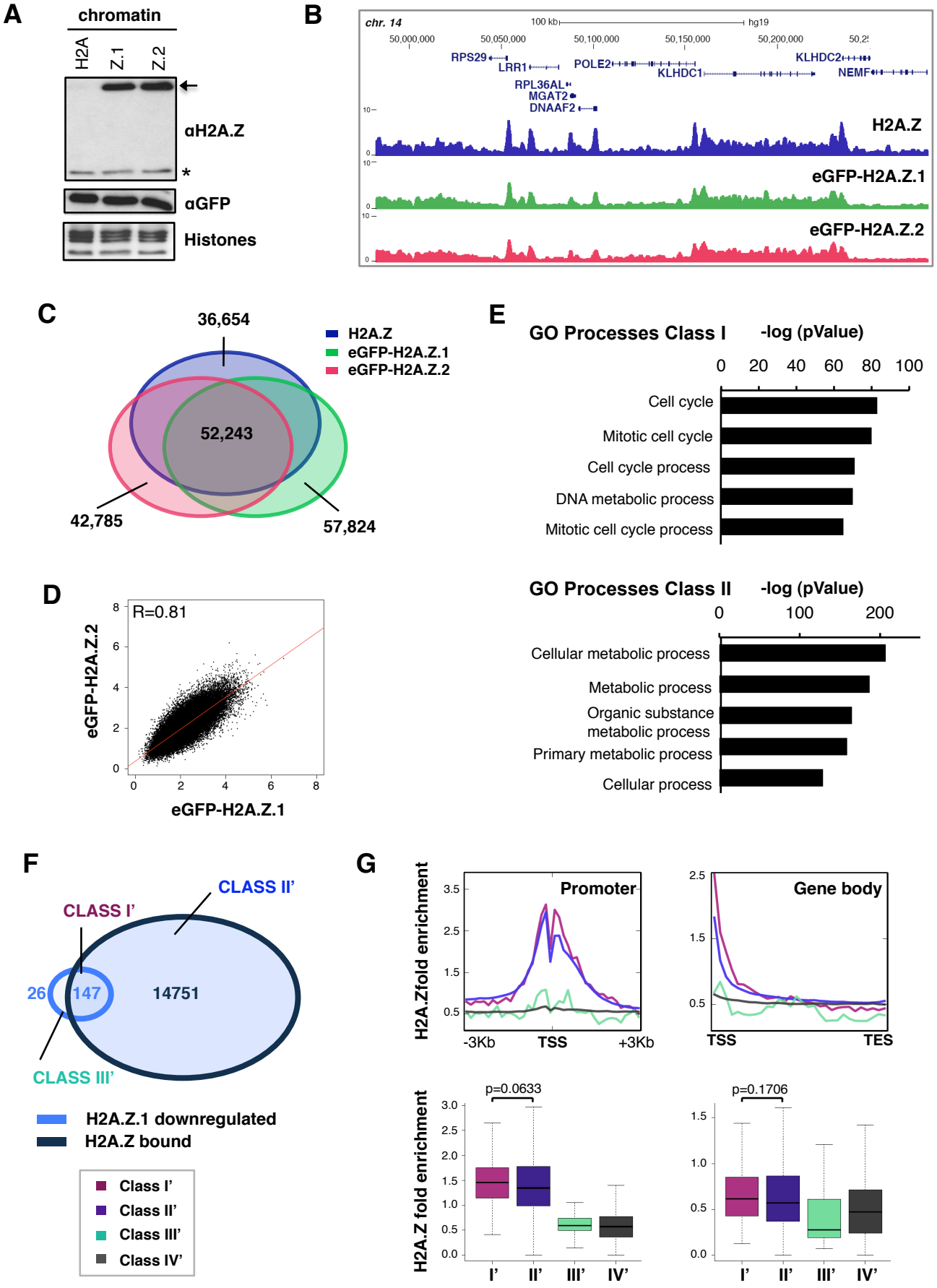
A
chromatin
H2A
Z.1
Z.2
αH2A.Z
*
αGFP
Histones
B
chr. 14
100 kb
hg19
50,000,000
50,050,000
50,100,000
50,150,000
50,200,000
RPS29
LRR1
POLE2
KLHDC1
KLHDC2
NEMF
RPL36AL
MGAT2
DNAAF2
H2A.Z
eGFP-H2A.Z.1
eGFP-H2A.Z.2
C
36,654
H2A.Z
eGFP-H2A.Z.1
eGFP-H2A.Z.2
52,243
42,785
57,824
D
R=0.81
eGFP-H2A.Z.2
eGFP-H2A.Z.1
E
GO Processes Class I
-log (pValue)
Cell cycle
Mitotic cell cycle
Cell cycle process
DNA metabolic process
Mitotic cell cycle process
GO Processes Class II
-log (pValue)
Cellular metabolic process
Metabolic process
Organic substance metabolic process
Primary metabolic process
Cellular process
F
CLASS I'
CLASS II'
CLASS III'
26
147
14751
H2A.Z.1 downregulated
H2A.Z bound
Class I'
Class II'
Class III'
Class IV'
G
H2A.Zfold enrichment
Promoter
Gene body
-3Kb
TSS
+3Kb
TSS
TES
H2A.Z fold enrichment
p=0.0633
p=0.1706
I'
II'
III'
IV'

Figure S4. H2A.Z.1 and H2A.Z.2 ChIP-seq analysis. Related to Figure 4.

(A) Immunoblots of chromatin extracts from SK-mel147 cells expressing eGFP-tagged H2A or H2A.Z isoforms with antibodies against H2A.Z and GFP. eGFP-H2A served as a control for specificity of H2A.Z and its expression is visualized only by GFP immunoblot. Arrow indicates ectopic H2A.Z isoforms, asterisk indicates endogenous H2A.Z. Core histones served as loading control. Note that tagged histones are expressed to a comparable extent and similarly incorporarted into chromatin.

(B) UCSC genome browser (GRCh37/hg19) capture of ~150Kb region of human chromosome 14. Read counts (normalized fold enrichment of ChIP over input DNA) for H2A.Z, eGFP-H2A.Z.1 and eGFP-H2A.Z.2 are shown. RefSeq annotated genes are displayed above. This genomic region was chosen to represent at least one Class I genes (*POLE2*) and one Class II gene (*KLHDC1*).

(C) Venn diagram representing the overlap of the genomic regions bound by H2A.Z, eGFP-H2A.Z.1 and eGFP-H2A.Z.2 (total number of peaks indicated).

(D) Enrichment correlation plot of eGFP-H2A.Z.1 and eGFP-H2A.Z.2 within significantly enriched H2A.Z regions; Spearman correlation (R=0.81).

(E) Functional annotation of Class I and Class II genes. Enriched groups are ranked by the most significant p value; analysis performed with MetaCore.

(F) Venn diagram displaying the intersection of H2A.Z.1 downregulated genes and H2A.Z targets identified by ChIP-seq in SK-mel147. Classes of genes were defined as follows: Class I' (downregulated in H2A.Z.1 knock down and bound by H2A.Z, purple); Class II' (bound by H2A.Z but whose expression is unaffected by H2A.Z.1 knock down, blue); Class III' (downregulated in H2A.Z.1 knock down but not bound by H2A.Z, green); Class IV' (not affected by H2A.Z.1 knock down and not bound by H2A.Z, grey).

(G) H2A.Z fold enrichment over input at the promoter and gene body (with corresponding boxplots) of Classes I', II', III', IV'. Note that H2A.Z.1 Class I' genes do not show increased promoter occupancy and decreased gene body occupancy (as compared to Class II') like H2A.Z.2 Class I genes (as compared to Class II). Statistical significance was determined by Mann-Whitney test.

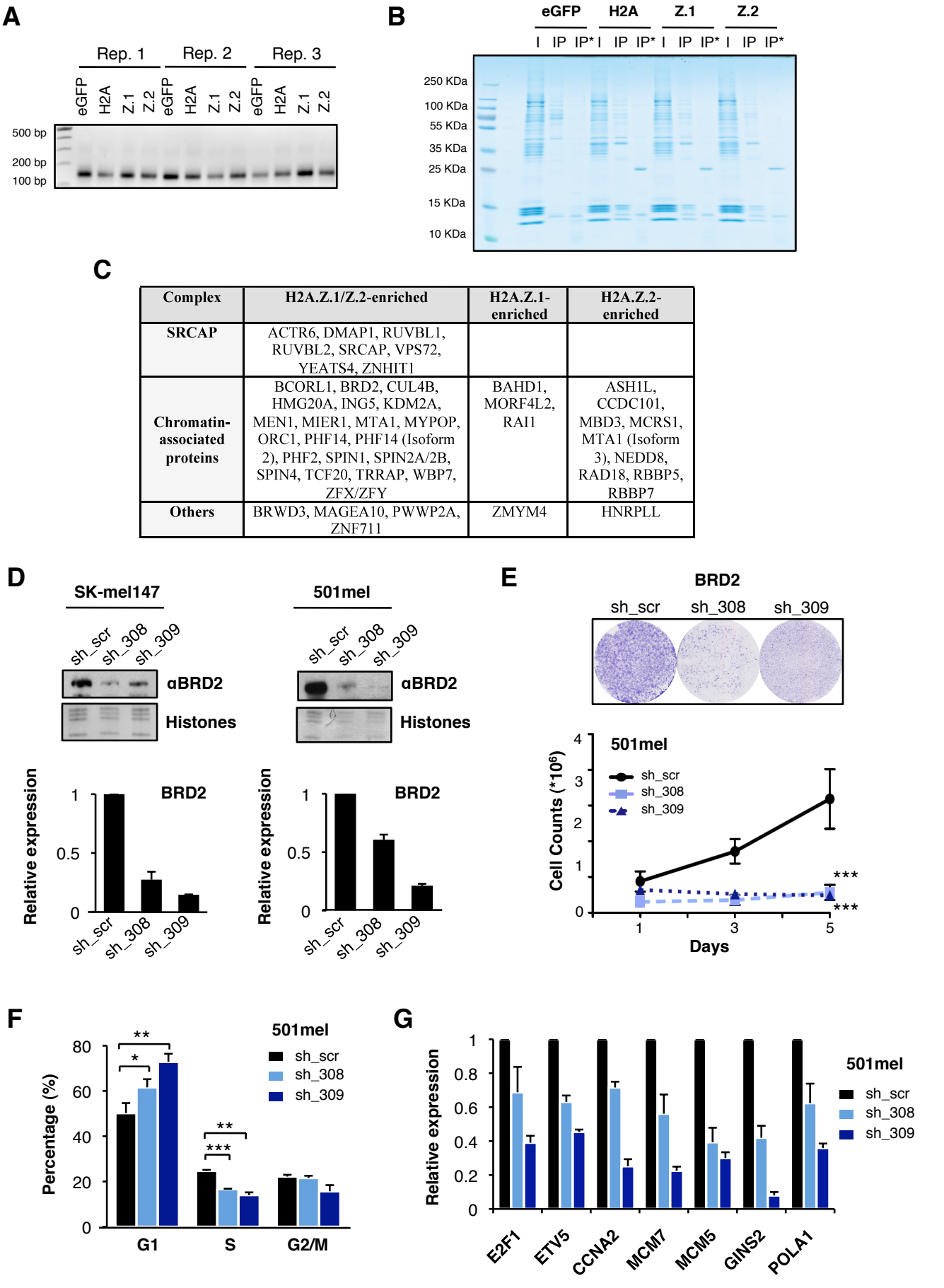

Complex	H2A.Z.1/Z.2-enriched	H2A.Z.1-enriched	H2A.Z.2-enriched
SRCAP	ACTR6, DMAP1, RUVBL1, RUVBL2, SRCAP, VPS72, YEATS4, ZNHIT1		
Chromatin-associated proteins	BCORL1, BRD2, CUL4B, HMG20A, ING5, KDM2A, MEN1, MIER1, MTA1, MYPOP, ORC1, PHF14, PHF14 (Isoform 2), PHF2, SPIN1, SPIN2A/2B, SPIN4, TCF20, TRRAP, WBP7, ZFX/ZFY	BAHD1, MORF4L2, RAI1	ASH1L, CCDC101, MBD3, MCRS1, MTA1 (Isoform 3), NEDD8, RAD18, RBBP5, RBBP7
Others	BRWD3, MAGEA10, PWWP2A, ZNF711	ZMYM4	HNRPLL

Figure S5. BRD2 interacts with H2A.Z-containing nucleosomes in melanoma cells and controls cellular proliferation. Related to Figure 5.

(A) Ethidium bromide-stained agarose gel showing complete mononucleosomal digestion for eGFP-histone expressing SK-mel147 cells. Shown are three replicates used for label-free MS quantification of eGFP-H2A, eGFP-H2A.Z.1 and eGFP-H2A.Z.2 immunoprecipitations (related to **Figure 5A**).

(B) Coomassie-stained SDS-PAGE gel of mononculeosome IP experiments (GFP-trap beads) for MS quantification experiments (related to **Figure 5A**). Loaded are input (I) and IP material before (IP) and after (IP*) tryptic digest.

(C) Summary of H2A.Z.1- and/or H2A.Z.2-nucleosome enriched interaction partners as compared to H2A-associated factors (see **Figure 5A** for Volcano plots and applied threshold). Note: some isoform specific-enriched proteins were also found enriched with the other isoform, but did not meet the stringent threshold criteria. Therefore we cannot exclude the possibility that these proteins interact with both H2A.Z.1 and H2A.Z.2.

(D) (Top) immunoblot (whole-cell extracts) and qRT-PCR (bottom) from SK-mel147 and 501mel melanoma cells stably transduced with non-targeting scrambled (sh_scr) control, or BRD2 shRNAs (sh_308, sh_309). For qRT-PCR, values are normalized to GAPDH, and relative to scrambled shRNA. Mean ± SD is shown ($n \geq 3$). For immunoblot, histones used for loading.

(E) Colony formation assay (top) and proliferation assay (bottom) of 501mel cells expressing BRD2 shRNAs as shown. 501mel cells were counted up to 5 days after plating and proliferation curves of control and BRD2-depleted cells are represented. Mean ± SD is shown ($n \geq 2$). Two-way ANOVA.

(F) Percentage of 501mel cells in G1, S or G2/M phases, as revealed by PI incorporation. Values are mean ± SD ($n \geq 3$); unpaired Student's test (two-tailed).

(G) Expression of a handful of Class I genes was analyzed by qRT-PCR upon BRD2 knock down. Expression is shown normalized to GAPDH and relative to scrambled shRNA. Mean ± SD is shown ($n \geq 3$).

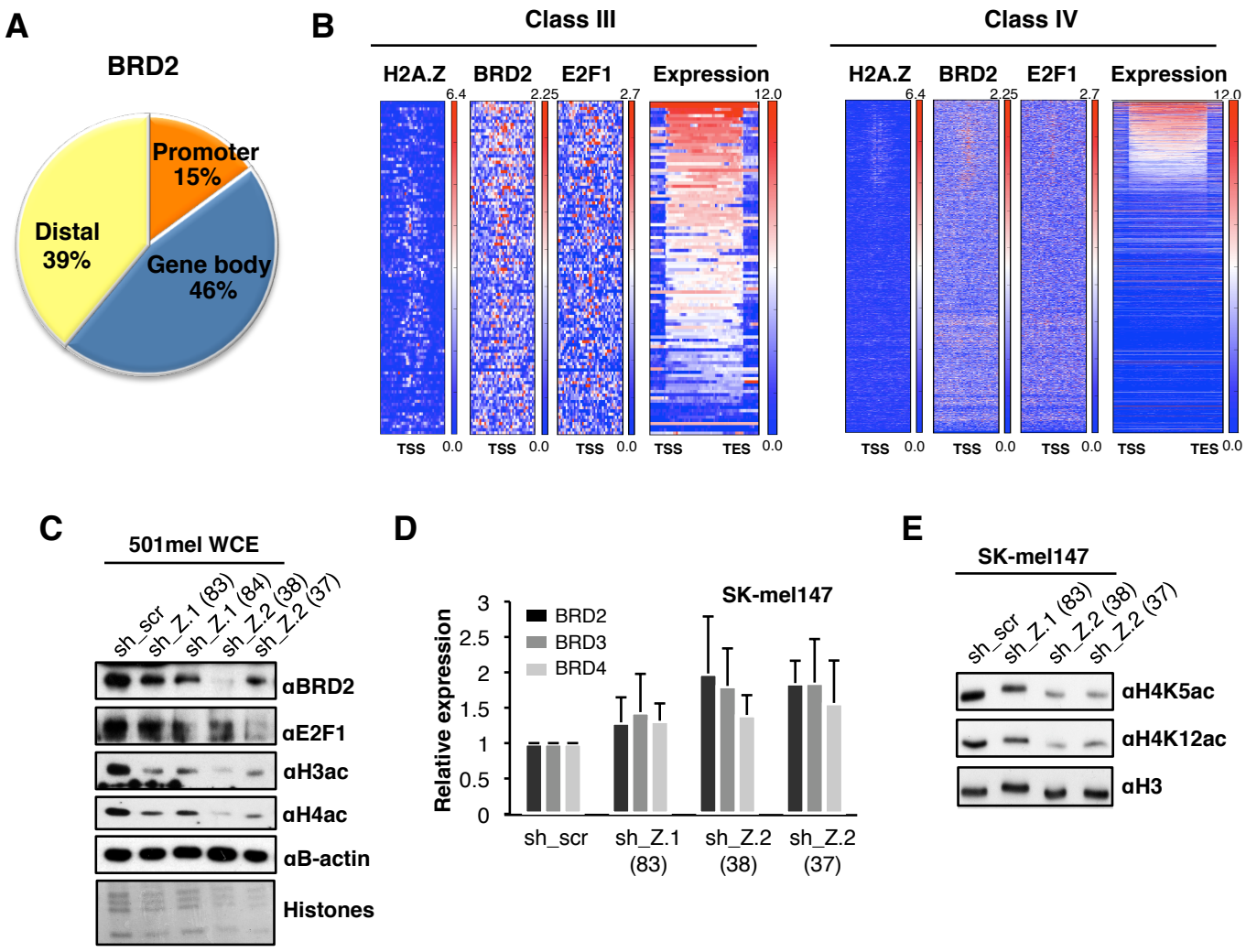

Figure S6. Characterization of the H2A.Z-BRD2-E2F axis in melanoma cells. Related to Figure 6.

(A) Pie chart displaying the percentages of BRD2 peaks occupying promoters, gene bodies and distal regions. Promoters: -3Kb < TSS < +1Kb; Gene bodies: from +1Kb > TSS to TES; all other regions defined as distal. (TSS: Transcription Start Site; TES: Transcription End Site).

(B) Heatmaps of promoters (-3Kb, +3Kb) of Class III and Class IV genes based on H2A.Z, BRD2 and E2F1 fold enrichment over input, and ranked by expression level. Expression is indicated as log2 RNA-seq signal.

(C) Whole-cell extracts from control and H2A.Z.1 or H2A.Z.2-depleted 501mel cells were immunoblotted for BRD2, E2F1 and H4ac. GAPDH as loading control.

(D) qRT-PCR of BRD2, BRD3, BRD4 mRNA levels in SK-mel147 cells stably transduced with scrambled and H2A.Z.1 or H2A.Z.2 shRNAs. Values normalized to GAPDH and relative to scrambled shRNA; mean ± SD (n≥3).

(E) Acid extracted histones from control, H2A.Z.1, and H2A.Z.2 knock down SK-mel147 cells were immunoblotted for histone H4 acetylated on lysines 5 and lysine 12 (H4K5ac and H4K12ac, respectively). Histone H3 was used as loading control (related **F**).

Vardabasso et al_Suppl. Figure 7

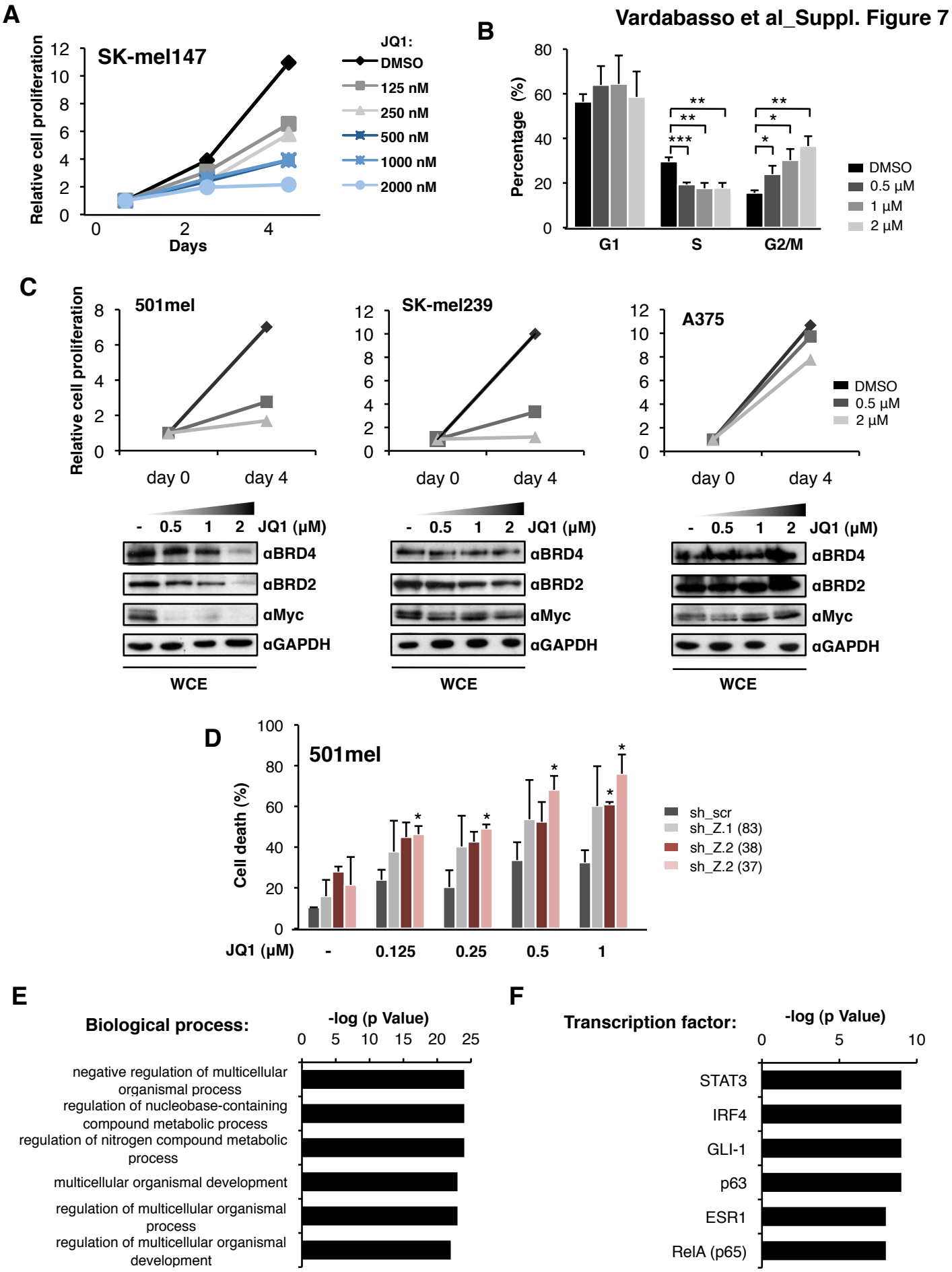

Figure S7. H2A.Z.2 deficiency cooperates with BETi to induce melanoma cell death. Related to Figure 7.

(A) SK-mel147 cells were exposed to increasing doses of JQ1 as indicated, and cells were counted 2 and 4 days after exposure to the drug. Normalized proliferation curves are represented.

(B) Percentage of SK-mel147 cells in G1, S, and G2/M phases via flow cytometry of PI stained cells upon 4 days of JQ1 treatment is shown. Values are mean ± SD (n≥3); unpaired Student's test (two-tailed).

(C) Sensitivity of metastatic melanoma lines to JQ1. Cells exposed to increasing amounts of JQ1 were counted after 4 days of treatment. Normalized proliferation curves are represented (upper panel). Immunoblots of whole-cell extracts for BRD2, BRD4, Myc and GAPDH as loading control are shown below each corresponding cell line (lower panel).

(D) 501mel ($BRAF^{V600E}$-mutant) melanoma cells were infected with scrambled and H2A.Z.1 or H2A.Z.2 shRNAs and subsequently exposed to increasing doses of JQ1. Bar graphs represent the percentage of dead cells (Annexin V positive) upon 4 days treatment. Values are mean ± SD (n≥3). Unpaired Student's test (two-tailed).

(E) Functional annotation and TF regulation of genes downregulated in SK-mel147 cells treated with 1μM JQ1 for 6 hours (logFC<-1). Enriched groups are ranked by the most significant p value. All analyses performed with MetaCore.

SUPPLEMENTAL TABLES

Table S1. Microarray data of H2A.Z.1 and H2A.Z.2 knockdown in SKmel-147 and WM266-4 melanoma cell lines (Related to Figures 3, S3).

Table S2. Classes of genes as defined by H2A.Z.2 regulation and H2A.Z ChIP-seq (Related to Figures 4, S4).

Table S3. Classes of genes as defined by H2A.Z.1 regulation and H2A.Z ChIP-seq (Related to Figures 4, S4).

Table S4. RNA-seq data for genes downregulated upon JQ1 treatment in SK-mel147 cells (Related to Figures 7, S7).

EXTENDED EXPERIMENTAL PROCEDURES

Cell culture, plasmids and infections

SK-mel147, WM266-4, 501mel, A375, SK-mel2, SK-mel28 and HeLa cells were maintained in DMEM supplemented with 10% fetal bovine serum (FBS) and 1% antibiotics. SK-mel239, SK-mel5 and M14 cells were grown in RPMI; WM165-1, WM115, WM1789 and WM39 in Tu2% media (80% MCDB 153 media, 20% Leibovitz's L-15 media, 2% FBS, 5 μg ml^{-1} bovine insulin, 1.68 mM CaCl2). Human melanocytes were cultured in Melanocyte Growth Media 254 supplemented with Human Melanocyte Growth Supplement (Life Technologies). Lentiviral plasmids encoding shRNAs against H2A.Z.1, H2A.Z.2 and BRD2 were obtained from Open Biosystems (Thermo Fisher Scientific, RHS4533-EG3015-NM_002106, RHS4533-EG94239-NM_012412 and RHS4533-EG6046-NM_005104 respectively). sh_scrambled and sh_luciferase–expressing cells were used as controls. shRNA sequences are listed below. eGFP-fused complementary DNA (cDNAs) encoding H2A, H2A.Z.1 and H2A.Z.2 were cloned into the lentiviral vector VIRSP (gift of S.A. Aaronson lab). FLAG-fused cDNAs encoding H2A.Z.1 and an shRNA-resistant form of H2A.Z.2 were bought from Geneart (Invitrogen) and cloned into the lentiviral vector NSBI (gift of S.A. Aaronson lab). Infections were performed using standard procedures (Kapoor et al., 2010).

shRNAs used in this study:

shRNA ID	Target sequence	Catalog No.*
H2A.Z.1		
sh_Z.1 (83)	5' - AAACCCAGGGCTGCCTTGGAAAAG - 3'	TRCN0000072583
sh_Z.1 (84)	5' - AAACCCAGGGCTGCCTTGGAAAAG - 3'	TRCN0000072584
H2A.Z.2		
sh_Z.2 (36)	5' - AAACCCAGGGCTGCCTTGGAAAAG - 3'	TRCN0000106836
sh_Z.2 (37)	5' - AAACCCAGGGCTGCCTTGGAAAAG - 3'	TRCN0000106837
sh_Z.2 (38)	5' - AAACCCAGGGCTGCCTTGGAAAAG - 3'	TRCN0000106838
BRD2		
sh_308	5' - AAACCCAGGGCTGCCTTGGAAAAG - 3'	TRCN0000006308
sh_309	5' - AAACCCAGGGCTGCCTTGGAAAAG - 3'	TRCN0000006309

* Purchased from Open Biosystems (Thermo Fisher Scientific)

Chromatin fractionation, acid extraction of histones and immunoblotting

Chromatin fractionation and acid extraction of histones were performed as described (Bernstein et al., 2008). Whole-cell extracts were generated by lysing cells directly in Laemmli loading buffer with subsequent boiling. Antibodies used are listed below.

Antibodies used in this study:

Antibody	Catalog No.
H2A.Z	Abcam ab4174
H2A.Zac	Abcam ab18262
H4ac	Millipore 06-866
H3ac	Millipore 06-599
H4K5ac	Abcam ab51997
H4K12ac	Abcam 46983
H3 C-terminal	Abcam ab1791 or Millipore 05-928
Rb	Santa Cruz sc-102
Phospho-Rb (Ser807/811)	Cell Signaling #9308
Cyclin A	Santa Cruz sc-239
Cyclin E	Santa Cruz sc-247
E2F1	Santa Cruz sc-193 or Invitrogen 33-7000
BRD2	Bethyl Laboratories A302-583A
BRD4	Bethyl Laboratories A301-985A50
Myc	Cell Signaling #5605
GFP	Roche 11814460001
B-actin	Sigma A5441
GAPDH	Santa Cruz sc-32233

RNA extraction and qRT-PCR

Total RNA was extracted using RNeasy Mini Kit (Qiagen). Reverse transcription was performed with First-strand cDNA Synthesis (OriGene). qPCR reactions were performed in triplicate on Stratagene Opticon 2 using Absolute Blue qPCR SYBR Green (Thermo Scientific). cDNA expression was normalized to GAPDH or B-actin levels. Each qPCR was performed on three independent biological replicates. Primer sequences are provided below.

Primers used in this study for RT-qPCR:

Gene ID	Primer name	Sequence
*H2A.Z.1**	Z.1_fw	5' – GGCAGGAAATGCATCAAAAG – 3'
	Z.1_rv	5' – TGGATGTGTGGAATGACACC – 3'
*H2A.Z.2**	Z.2_fw	5' – GAGCTGGCAGGTAATGCTTC – 3'
	Z.2_rv	5' – TTTGTGGATGTGAGGGATCA – 3'
CDKN1A	p21_fw	5' – CAGGGGACAGCAGAGGAAGA – 3'
	p21_rv	5' – TTAGGGCTTCCTCTTGGAGAA – 3'
CDKN2A	p16_fw	5' – GAAGGTCCCTCAGACATCCCC – 3'
	p16_rv	5' – CCCTGTAGGACCTTCGGTGAC – 3'
CDKN1B	p27_fw	5' – ATCACAAACCCCTAGAGGGCA – 3'
	p27_rv	5' – GGGTCTGTAGTAGAACTCGGG – 3'
E2F1	E2F1_fw	5' – ACGCTATGAGACCTCACTGAA – 3'

	E2F1_rv	5’ – TCCTGGGTCAACCCCTCAAG – 3’
E2F3	E2F3_fw	5’ – GTATGATACGTCTCTTGGTCTGC – 3’
	E2F3_rv	5’ – CAAATCCAATACCCCATCGGG – 3’
E2F6	E2F6_fw	5’ – TCCATGAACAGATCGTCATTGC – 3’
	E2F6_rv	5’ – TCCGTTGGTGCTCCTTATGTG – 3’
ETV1	ETV1_fw	5’ – CTGAACCCTGTAACTCCTTTCC – 3’
	ETV1_rv	5’ – AGACATCTGGCGTTGGTACATA – 3’
ETV5	ETV5_fw	5’ – TCAGCAAGTCCCTTTTATGGTC – 3’
	ETV5_rv	5’ – GCTCTTCAGAATCGTGAGCCA – 3’
MCM5	MCM5_fw	5’ – AGCATTCGTAGCCTGAAGTCG – 3’
	MCM5_rv	5’ – CGGCACTGGATAGAGATGCG – 3’
MCM7	MCM7_fw	5’ – ACGTCAGCGTCACTGGTATTT – 3’
	MCM7_rv	5’ – CTTCCAGGTAGGTTTCTGAGAGT – 3’
GINS2	GINS2_fw	5’ – CCCTGGTTTACCCGTGGAAG – 3’
	GINS2_rv	5’ – GAGCAGGCGACATTTCTGTCT – 3’
CCNA2	CCNA2_fw	5’ – CGCTGGCGGTACTGAAGTC – 3’
	CCNA2_rv	5’ – GAGGAACGGTGACATGCTCAT – 3’
CCNB2	CCNB2_fw	5’ –CCGACGGTGTCCAGTGATTT – 3’
	CCNB2_rv	5’ –TGTTGTTTTGGTGGGTTGAACT – 3’
POLA1	POLA1_fw	5’ – AAAGATCCATTGGAGCTTCACC – 3’
	POLA1_rv	5’ – TCAGCACGTTTAAGAGGAACAG – 3’
RAD51	RAD51_fw	5’ –CGAGCGTTCAACACAGACCA – 3’
	RAD51_rv	5’ – GTGGCACTGTCTACAATAAGCA – 3’
CENPE	CENPE_fw	5’ – GATTCTGCCATACAAGGCTACAA – 3’
	CENPE_rv	5’ – TGCCCTGGGTATAACTCCCAA – 3’
BRD2	BRD2_fw	5’ – AGGAGGGCTAGCTGGAGAAC – 3’
	BRD2_rv	5’ – CAAGTCCTTGCACTCTGCTG – 3’
ACTB	B-actin_fw	5’ – AGGGCATACCCCTCGTAGAT – 3’
	B-actin_rv	5’ – AGAAAATCTGGCACCACACC – 3’
GAPDH	GAPDH_fw	5’ – TTTGTCAAGCTCATTTCCTGG– 3’
	GAPDH_rv	5’ – TGATGGTACATGACAAGGTGC– 3’

*(Bonisch et al., 2012)

Fluorescent In Situ Hybridization (FISH)

FISH was performed as previously described (Faggioli et al., 2012) using two locus-specific probes for *H2AFZ* and *H2AFV*. For *H2AFZ* (chromosome 4): BAC clones RP11-626I16 and RP11-321M7; for *H2AFV* (chromosome 7): BAC clones RP11-302H15 and RP11-1005N1.

Genomic DNA extraction and qRT-PCR for copy number analysis

Genomic DNA was extracted using DNeasy Blood & Tissue Kit (Qiagen). qPCR reactions were performed as described above. *GNS* was used as a reference gene for normalization (Lazar et al., 2009). Each qPCR was performed on three independent biological replicates. Primer sequences are provided below.

Primers used in this study for copy number qPCR:

Genomic locus	Primer name	Sequence
H2AFZ (Z.1)	H2AFZ3'_fw	5' – TCCACTCTGGTGGATAAGTTCA – 3'
	H2AFZ3'_rv	5' – TTGGGCTATCTCACTTTGTTGA – 3'
H2AFV (Z.2)	H2AFV3'_fw	5' – CTGGCTGACTCCAGAGCCTA – 3'
	H2AFV3'_rv	5' – GAGACGGCGTTTTACCATGT – 3'
GNS	GNS_fw	5' – TCCAACTTTGAGCCCTTCTT – 3'
	GNS_rv	5' – CGTTCCATGGATGTTGAAGT – 3'

Cell proliferation, colony formation and flow cytometry

For DNA content analysis, floating cells were harvested and combined with trypsinized cells, washed with phosphate-buffered saline and stained with propidium iodide using the CycleTEST Plus DNA reagent kit (Becton Dickinson, BD). Synchronization of the cells at early S phase was obtained by double-thymidine block (21 hours first block, 5 hours release, 17 hours second block) using 2mM Thymidine (Sigma). For BrdU staining, cells were pulsed for 20' with 10μM BrdU and then processed with FITC BrdU Flow Kit (BD), according to manufacturer's instructions. For apoptosis analysis, cells were collected as described above, and subjected to Annexin V staining using the FITC Annexin V Apoptosis Detection Kit (BD), according to manufacturer's protocol. All FACS analyses were performed using BD Cell Quest 3.2 and FlowJo 6.7 softwares.

Microarray Analysis

Probeset expression values were calculated with the RMA function of the 'oligo' library. Control probes and probes with zero variance in expression across arrays were removed. Only probesets that exceeded a log2 expression level of 4 at least once in at least one experimental condition were kept for further analysis. Differential expression was tested using the 'limma' library. Based on the resulting test statistic (t) the local false discovery rate (lfdr) was determined using the 'locfdr' library. An average of two shRNAs per isoform (83 and 84 for H2A.Z.1; 37 and 38 for H2A.Z.2) was considered, relative to an average of two non-targeting control shRNAs (sh_scr and sh_luc) in SK-mel147. Two biological replicates were performed, and shown in the heatmap in **Figure 3A**. For WM266-4 cells, two shRNAs per isoform (83 and 84 for H2A.Z.1; 36 and 38 for H2A.Z.2) were considered, relative to an average of two controls (sh_scr and wild type cells). Time points taken for mRNA isolation were at eight days post infection for SK-mel147, and six days post infection for WM266-4.

RNA sequencing library preparation and analysis

Sequencing libraries were prepared following the Illumina TruSeq Stranded Total RNA library prep protocol, with Ribo-Zero (RS-122-2201 or -2202), starting from 300-500ng of DNase I-treated total

RNA, with the exception of 13 cycles of PCR amplification instead of 15. Amplified libraries were purified using AMPure beads, quantified by Qubit and qPCR, and visualized on an Agilent Bioanalyzer. Pooled libraries were loaded on high throughput HiSeq 2500 flow cells, using v3 reagents, and sequenced 50nt, paired-end. RNA reads were aligned to the GRCh37/hg19 human genome assembly using TopHat (version 2.0.12). Transcriptome assemblies in FPKM (fragments per kilo-base per million reads), and differential expression ratios were computed with Cufflinks (version 2.2.1). For each RNA sample two technical replicates were merged.

Cross-linked ChIP-seq and ChIP-qPCR

For BRD2 and E2F1, 1-3x10^7 cells (SK-mel147 and SK-mel147 stably expressing control or isoform-specific shRNAs) were cross-linked, with 1% formaldehyde for 10 min at 25°C. Cells were resuspended and lysed for 10min at 4°C with ChIP lysis buffer (50mM Hepes-KOH, pH7.6, 140mM NaCl, 1mM EDTA, 10% Glycerol, 0.5% Igepal, 0.25% TritonX), washed in ChIP wash buffer (10mM Tris-HCl, pH8, 200mM NaCl, 1mM EDTA, and 0.5mM EGTA) for 10min at 4°C and resuspended in ChIP shearing buffer (10mM Tris-HCl pH8, 100mM NaCl, 1mMEDTA, 0.5mM EGTA, 0.1% w/v deoxycholic acid, and 0.5% w/v Lauroylsarcosine). Cells were aliquoted in Covaris AFA microtubes (~6.6x10^6 cells in 130 ul per tube) and sonicated using a Covaris E220 (Intensity 2, DC 5%, CPB 200, duration 840sec). Fragment size (200-400bp) was evaluated using Agilent Bioanalyzer 2100. Samples were then diluted to 1.5ml, TritonX was added to a final concentration of 1%, and pre-cleared with 30ul of Dynal Magnetic beads for 20min at 4°C. The antibodies were coupled to the magnetic beads for 12 hours in blocking buffer (0.5% FBS in PBS), incubation was performed for 12-16 hours. Beads were subsequently washed 5 times using RIPA buffer (50mM Hepes-KOH, pH7.6, 300mM LiCl, 1mM EDTA, 1% NP-40 (IGEPAL), 0.7% Na-Deoxycholate) and once with Tris-EDTA (TE) buffer (50mM NaCl). Precipitated chromatin was eluted in 200ul of Elution buffer (50mM Tris-HCl pH8, 10mM EDTA, and 1% SDS), after 2 hours incubation at 65°C. Reverse cross-linking was carried out for 12 hours at 65°C. Chromatin was then treated with RNase A, for 2 hours at 37°C, and Proteinase K, at 56°C for 4 hours. DNA was purified with phenol/chloroform extraction followed by Chloroform/H2O extraction and MiniElute PCR purification tubes.

For ChIP-qPCR, immunoprecipitated DNA was used for qPCR essentially as described (Hasson et al., 2013). In some cases, different primer pairs were used to detect signal of BRD2 and E2F1 peaks within the same promoter region (B = BRD2, E = E2F1 in primer names). Primer sequences in the table below:

Primers used in this study for ChIP-qPCR:

Gene ID	Primer name	Sequence
CENPP	CENPP_B_fw	5' – GGCCTACCTCTTCCCGATAG – 3'
	CENPP_B_rv	5' – ACAGGGCCGTTTCCTAGTCT – 3'
	CENPP_E_fw	5' – CGTGAGCTCTGGGATGGT – 3'
	CENPP_E_rv	5' – CAGCTGTCACTCCGACCTG – 3'
RFC3	RFC3_B_fw	5' – GGACAGAGTTCCACACCTAGC – 3'
	RFC3_B_rv	5' – TTTGGCGTCACATCCAGATA – 3'
CDK1	CDK1_fw	5' – AAAGAAGAACGGAGCGAACA – 3'
	CDK1_rv	5' – GTCGGGAGAGTGTCGTCCTA – 3'
DEK	DEK_fw	5' – CGGCTCCCCAGAATCAAC – 3'
	DEK_rv	5' – GCATTCCCGCTCTCCTTC – 3'
EXOSC2	EXOSC2_B_fw	5' – AAGATGGCGATGGAGATGAG – 3'
	EXOSC2_B_rv	5' – TACCGCATGAATCCTGTGTC – 3'
	EXOSC2_E_fw	5' – AAGATGGCGATGGAGATGAG – 3'
	EXOSC2_E_rv	5' – TTAGTGTCGCGGCCCAGT – 3'
CASC5	CASC5_fw	5' – GGCTGTGACGCAATGTTATG – 3'
	CASC5_rv	5' – TTTCGACCGAATTTCCTCTG – 3'
USP1	USP1_B-fw	5' – GGCCTCAGCTCTACAGCATT – 3'
	USP1_B-rv	5' – GGGCTTTCAGTTCGGAGTC – 3'
	USP1_E2-fw	5' – CGTACGCTTTTCCCTCAACT – 3'
	USP1_E2-rv	5' – CTCGAGCCTCACACCCTTT – 3'

ChIP-seq data processing and quality control (QC)

The number of reads obtained, aligned and processed is provided below. ChIP-seq reads were analyzed with fastqc and the NGS-QC tools for quality control. Reads were aligned to the human genome assembly GRCh37/hg19 using Bowtie short read aligner (version 0.12.7) with the following parameters: seed of 45 bp, maximum two mismatches, suppression (*m*)=20, --best option and reported alignments (*k*)=1.

Number of sequenced and processed ChIP-seq reads:

Sample	Sequenced reads	Aligned reads (hg19)	Number of Peaks
SK-mel147 Input	130,436,332	108,260,574	N/A
SK-mel147 H2A.Z	60,161,749	54,021,644	88,897
SK-mel147-eGFP-H2A	50,325,516	43,976,424	N/A
SK-mel147-eGFP-H2A.Z.1	116,416,179	83,201,544	110,067
SK-mel147-eGFP-H2A.Z.2	105,767,449	80,687,891	95,028
SK-mel147 BRD2	61,173,148	50,595,543	27,465
SK-mel147 E2F1	33,584,097	28,291,563	24,748
Melanocytes Input	129,673,301	108,547,296	N/A
Melanocytes H2A.Z	77,841,188	68,183,226	N/A

Significant peak calling was performed using MACS2 (version 2.1.0). For H2A.Z the --broad option was used, and the options --nomodel --extsize 300 were added. H2A.Z peaks were called with a q-value cutoff of 5x10^-3. BRD2 and E2F1 were called with a p-value cutoff of 1x10^-2. The rest of the parameters were kept as default values. Pileups were generated using MACS2 (Fold enrichment over Input control, --SPMR option). Plots for average fold enrichment patterns and heat maps were generated using DeepTools. Correlation plots and correlation analyses were performed with R.

Promoter and Gene Body (Metagene) analysis

Promoters (from -3Kb to +1Kb relative to the TSS), genes (+1Kb to TES) and distal regions (regions that do not overlap with promoters or genes) were defined according to the human hg19 (GRCh37.p13) gene annotation of Ensembl (gene database version 75). The percentage of peaks within each category was calculated using BedTools and in house scripts. RNA-seq heatmaps were generated using DeepTools, the log2 (signal+1) was plotted. Promoters were plotted +/- 3Kb around TSS. Gene bodies were scaled to a relative size of 4.5Kb from TSS to TES. Both regions were divided in 150bp non-overlapping bins. Boxplots were generated plotting the total enrichment within promoters or genes using R. Total enrichment values were calculated with DeepTools for promoters (H2AZ promoters +/- 2.3Kb around TSS; BRD2 promoters +/- 1.2Kb around TSS; E2F1 promoters +/- 0.7Kb around TSS) and gene bodies (from TSS to TES for all marks).

Mononucleosome Immunoprecipitation (IP)

Cells were lysed, nuclear pellets isolated and digested with MNase (SIGMA) as described (Sansoni et al., 2014) with the following adjustments. To check for successful chromatin digestion, the precipitated DNA was analyzed on ethidium-bromide stained agarose gel or a DNA 1000 BioAnalyzer chip (Agilent). For label-free mass spectrometry, the supernatant (S1) that predominantly contained mononucleosomes ($2.4x10^8$ cells per cell line) was prepared and used as input for three replicate IPs with GFP-trap beads (Chromotek). Briefly, 25 µl slurry beads per IP were equilibrated in EX100 buffer and then incubated with mononucleosomes of $8x10^7$ cells for 2.5 h at 4°C (rotating). Beads were washed twice in wash-buffer 1 (10mM Tris-HCl, pH 7.5, 150mM NaCl, 1mM DTT, 1xCPI), followed by 2 washes in wash-buffer 2 (10mM Tris-HCl, pH 7.5, 150mM NaCl, 0.1% NP-40). Samples were either boiled with 1x Laemmli buffer for immunoblot analysis or digested overnight at RT with trypsin (Promega) for LC-MS/MS analysis. Tryptic digest was performed as described (Hubner et al., 2010) and the resulting peptides were purified and concentrated on activated C18 StageTips (Rappsilber et al., 2007).

LC-MS/MS Analysis

Peptides were eluted from the C18 StageTips according to standard protocol (Rappsilber et al., 2007). Samples were analyzed by reversed-phase liquid chromatography on an EASY-nLC 1000

system (Thermo Fisher Scientific, Odense, Denmark) directly coupled to a Q Exactive mass spectrometer (Thermo Fisher Scientific) using an nanoelectrospray source (Proxeon Biosystems, now Thermo Fisher Scientific). HPLC columns of 20 cm length and an inner diameter of 75 µm were in-house packed with ReproSil-Pur 120 C18-AQ 1.9 µm particles (Dr. Maisch GmbH, Germany). Peptide mixtures were separated using linear gradients of 140 minutes (total run time + washout) and a two buffer system: buffer A++ (0.1% formic acid) and buffer B++ (80% acetonitrile in 0.1% formic acid). The flowrate was set to 250 nl/min and the column was heated to 50°C using a column oven (Sonation GmbH, Germany). Peptides eluting from the column were directly sprayed into the mass spectrometer; with the spray voltage set to 2.4 kV and the capillary temperature set to 250°C. The mass spectrometer was operated in a data-dependent mode acquiring survey scans at a resolution of 70000 with an AGC target of 3E06 ions and a maximum ion injection time of 20ms. Subsequently, the top 10 most abundant peaks were selected for fragmentation with an isolation window of 2m/z and fragmented by higher energy collisional dissociation (HCD) with a normalized collision energy of 25. Fragmentation spectra were acquired at a resolution of 17500 with a target value of 1E05 ions and 120 msec as maximum ion injection time. To minimize re-sequencing of peptides, dynamic exclusion was enabled within a time window of 20 sec.

Raw MS Data analysis

MS raw files were processed using MaxQuant (Cox and Mann, 2008) version 1.3.9.20, leading to the identification of roughly 1600 proteins in each technical replicate. MS/MS spectra were searched against a human sequence database obtained from Uniprot on 2/25/2012 using the Andromeda search engine (Cox et al., 2011). Cysteine carbamidomethylation was set as a fixed modification; N-terminal acetylation and methionine oxidation were set as variable modifications. Trypsin was chosen as specific enzyme, with 2 maximum missed cleavages allowed. Peptide and protein identifications were filtered at a 1% FDR. Label-free quantification was enabled, with a minimum ratio count of 1. The match between runs option was enabled, while the requantify option was disabled. All other parameters were left at standard settings.

MS Data analysis

Label-free mononucleosome IP experiments were analyzed using the freely available Perseus software (version 1.3.10.0), part of the MaxQuant environment. Identified proteins were filtered as follows: contaminants, hits to the reverse database and proteins only identified with modified peptides were eliminated Additionally, at least 2 unique or razor peptides were required per protein. Label-free intensities were logarithmized, then samples were grouped into triplicates and identifications were filtered to require three valid values in at least one group. To enable statistical analysis, missing values were imputed with values representing a normal distribution around the detection limit of the mass spectrometer. To that end, mean and standard deviation of the real distribution of intensities

were determined, then a new distribution with a downshift of 1.8 standard deviations and a width of 0.3 standard deviations was created. Interacting proteins were identified by performing two-sample *t*-tests essentially as previously described (Hubner et al., 2010). First, background binders were removed by keeping only proteins that were enriched (*t*-test difference > 0) in the eGFP-histone IPs (eGFP-H2A, -H2A.Z.1, -H2A.Z.2) compared to the control IP (eGFP). For the remaining proteins two sample *t*-tests were applied to compare eGFP-H2A.Z.1 respectively eGFP-H2A.Z.2 to eGFP-H2A. The respective *p*-values and *t*-test differences were plotted against each other in volcano plots using R (version 3.0.2), to visualize interacting proteins specifically enriched on H2A.Z.1- or H2A.Z.2-containing mononucleosomes versus H2A-containing mononucleosomes. Proteins with a *p*-value ≤ 0.1 and a *t*-test difference ≥ 1 were selected as promising candidates.

BRD2 Immunohistochemistry

Formalin-fixed paraffin-embedded (FFPE) tissue sections of benign intradermal nevi, primary tumors, and metastatic resections were obtained from Mount Sinai Hospital Department of Pathology, Dermatopathology Division. The Institutional Review Board at the Icahn School of Medicine at Mount Sinai approved this study (project number HSD08-00565). Inclusion criteria for benign nevi were patients 30 to 65 years old and intradermal nevi of non-facial and non-ungual origin. Only primary tumors described on pathology reports as non-lentiginous and non-desmoplastic thick melanoma (>1 mm) were included. Average thickness of primary tumors was 4.4mm. Slides containing FFPE tissue sections were manually deparaffinized through xylene and graded ethanol washes. Subsequent steps were performed using the automated Bond-RX system (Leica Microsystems, Buffalo Grove, IL) as follows: (1) heat-induced epitope retrieval (antigen unmasking) with Bond Epitope Retrieval Solution 1 (pH 6.0; Leica Microsystems) for 20 minutes at 100°C; (2) incubation with monoclonal anti-BRD2 (Abcam, ab139690, 1:250) or anti-H3 (Abcam, ab1791, 1:300) with Bond Primary Antibody diluent (Leica Microsystems) for 30 minutes at ambient temperature; (3) Bond Polymer Refine Red Detection kit (Leica Microsystems) including Post Primary alkaline phosphatase reagent containing anti-rabbit IgG for 20 minutes, Mixed Red Refine as a chromogen for 15 minutes, and Hematoxylin counterstaining for 5 minutes. After counterstaining, slides were manually washed through graded ethanol and xylene, and mounted using Permount (Fisher Cat. #SP15-100) and 24x50 Coverslips (Fisher Cat. #12-545-88).

IHC Scoring and Statistical Analysis

Slides were scored by two independent dermatopathologists (J.L.Y and R.S.) in a blinded fashion. Positive staining was identified as intense pink nuclear staining of dermal melanocytic cells in intradermal nevi or neoplastic cells in primary and metastatic tissues. Tissues with aberrant H3 staining were excluded from analysis. Scoring of tissues was based on percentage of positively stained nuclei and staining intensity. Percentage of stained nuclei was quantified on a 4-point scale

(1: 0-25%, 2: 25-50%, 3: 50% - 75%, 4: 75% - 100%). Staining intensity was quantified on a 3-point scale (1: None to low, 2: Medium, 3: High). Scores for staining intensity and nuclei were multiplied to obtain a single arbitrary unit (A.U.) for each tissue per pathologist. The averaged A.U. per tissue was analyzed for statistical significance of BRD2 between nevi, primary tumors, and metastases using non-parametric Kruskal-Wallis one-way ANOVA and two-tailed Mann-Whitney tests.

SUPPLEMENTAL REFERENCES

Bernstein, E., Muratore-Schroeder, T.L., Diaz, R.L., Chow, J.C., Changolkar, L.N., Shabanowitz, J., Heard, E., Pehrson, J.R., Hunt, D.F., and Allis, C.D. (2008). A phosphorylated subpopulation of the histone variant macroH2A1 is excluded from the inactive X chromosome and enriched during mitosis. Proc Natl Acad Sci U S A *105*, 1533-1538.

Bonisch, C., Schneider, K., Punzeler, S., Wiedemann, S.M., Bielmeier, C., Bocola, M., Eberl, H.C., Kuegel, W., Neumann, J., Kremmer, E.*, et al.* (2012). H2A.Z.2.2 is an alternatively spliced histone H2A.Z variant that causes severe nucleosome destabilization. Nucleic Acids Res.

Cox, J., and Mann, M. (2008). MaxQuant enables high peptide identification rates, individualized p.p.b.-range mass accuracies and proteome-wide protein quantification. Nat Biotechnol *26*, 1367-1372.

Cox, J., Neuhauser, N., Michalski, A., Scheltema, R.A., Olsen, J.V., and Mann, M. (2011). Andromeda: a peptide search engine integrated into the MaxQuant environment. J Proteome Res *10*, 1794-1805.

Faggioli, F., Wang, T., Vijg, J., and Montagna, C. (2012). Chromosome-specific accumulation of aneuploidy in the aging mouse brain. Hum Mol Genet *21*, 5246-5253.

Hasson, D., Panchenko, T., Salimian, K.J., Salman, M.U., Sekulic, N., Alonso, A., Warburton, P.E., and Black, B.E. (2013). The octamer is the major form of CENP-A nucleosomes at human centromeres. Nat Struct Mol Biol *20*, 687-695.

Hubner, N.C., Bird, A.W., Cox, J., Splettstoesser, B., Bandilla, P., Poser, I., Hyman, A., and Mann, M. (2010). Quantitative proteomics combined with BAC TransgeneOmics reveals in vivo protein interactions. J Cell Biol *189*, 739-754.

Lazar, V., Ecsedi, S., Szollosi, A.G., Toth, R., Vizkeleti, L., Rakosy, Z., Begany, A., Adany, R., and Balazs, M. (2009). Characterization of candidate gene copy number alterations in the 11q13 region along with BRAF and NRAS mutations in human melanoma. Mod Pathol *22*, 1367-1378.

Rappsilber, J., Mann, M., and Ishihama, Y. (2007). Protocol for micro-purification, enrichment, pre-fractionation and storage of peptides for proteomics using StageTips. Nat Protoc *2*, 1896-1906.

Sansoni, V., Casas-Delucchi, C.S., Rajan, M., Schmidt, A., Bonisch, C., Thomae, A.W., Staege, M.S., Hake, S.B., Cardoso, M.C., and Imhof, A. (2014). The histone variant H2A.Bbd is enriched at sites of DNA synthesis. Nucleic Acids Res.